An Active 3-D Scanning System Based on Volumetric and Photometric Calibration

Irfanud Din[1], Hafeez Anwar[2] and Kang Park[3]
[1] Dept. of Electronics Engineering, Incheon National University, Incheon, South Korea
[2] Ph.D. School of Informatics, Vienna University of Technology, Vienna, 1040, Austria
[3]Dept. of Mechanical Engineering, Myongji University, Yongin,Gyeonggi-Do, South Korea
Email: kang@mju.ac.kr

Abstract: In this paper, we present a simple three dimensional (3-D) shape measurement system based on simple volumetric and photometric calibration. A liquid crystal display (LCD) projector is used to project a set of fringe patterns on to the surface of an object. The projected patterns are captured with a charge couple device (CCD) camera. The depth of the object causes phase variations in the projected patterns. These phase variations are used to construct a dense 3-D point cloud representing the surface of the object using homography, phase unwrapping, and phase map to coordinate conversion. The measuring volume is defined and calibrated using calibration boards. This measuring volume reduces the complexity of the system and enables it to measure 3-D objects without projector calibration. Photometric calibration is used to construct a lookup table that maps the captured intensity to the projected intensity value. The experimental results described are obtained using an HS200 LG LCD projector and a UEYE CCD camera with 1024 × 768 resolutions.
[Irfanud Din, Hafeez Anwar and Kang Park. **An Active 3-D Scanning System Based on Volumetric and Photometric Calibration.** *Life Sci J* 2013; 10(2):1970-1976]. (ISSN: 1097-8135). http://www.lifesciecensite.com. 278

Key words: Fringe projection, Homogrophy, Phase unwrapping, 3-D shape masurement

INTRODUCTION

The importance of three dimensional (3-D) object scanning has increased tremendously over the past decade as a result of its many valuable applications in the fields of medical diagnostics, dentistry, military, machine vision, robotics, large infrastructure inspection, etc. All of these applications are based on the 3-D point cloud calculated from the object. The quality of the scanning method is strongly dependent on the accuracy and speed. Even though there is a tradeoff between speed and accuracy, an accurate 3-D coordinate reconstruction within a reasonable scanning time is needed. An accurate point cloud can be obtained using the coordinate measurement machine (CMM). However, because of time-consuming nature of point-by-point scanning, this method is unacceptable for various applications.

Optical noncontact 3-D shape measurement techniques are used to extract the geometry information of an object with high speed and high accuracy. These techniques can be divided into two types: active 3-D scanning [1] [2], and passive 3-D scanning [3] [4]. Active scanning methods use structured illuminations or laser scanning whereas passive scanning methods are based on a stereo vision system. The major problem with stereo vision is its low accuracy. Because of their noncontact nature, laser scanners are widely used in dental and others applications. Line-by-line scanning remains a drawback of laser scanners, however. In most conventional vision systems, the accuracy has been fairly low but these systems are very sensitive to environmental changes [5] [6].

The digital fringe pattern projection method is advantageous because it offers high precision, high resolution, full field measurement, and easy implementation [3]. To scan the 3-D profile of an object, different methods have been proposed by researchers. [7] used gray-scale structured lighting for recovery of 3-D surface shape. He used 32 phase-shifted images to scan a single object. Because each image consists of a single sinusoidal pattern, the extracted phase need not be unwrapped, but projecting and capturing 32 images makes this method very time consuming. The coded structured light technique [8], which is based on projecting coded pattern and capturing the illuminated scene from a different view, is another reliable 3-D scanning technique. Patterns are designed in a special way and a set of pixels is assigned a code word. Encoding the patterns and detecting the code words makes this process more complex. [9] used a strip shifting pattern method for 3-D reconstruction. The distortion of the strip shadow on the object is used to obtain 3-D information on the object surface. Li's method is fast and low cost but the camera and the projector both need to be calibrated.

The moiré techniques [10] [12] [12] are useful for objects with relatively large flat surfaces and small depth variations. They are mostly used for repeated measurements and they provide information regarding the whole surface. A prior calibration must, however, be carried out. The limitations of moiré methods include implementation complexity, the need for a high power light source, and the inability to measure large

objects.

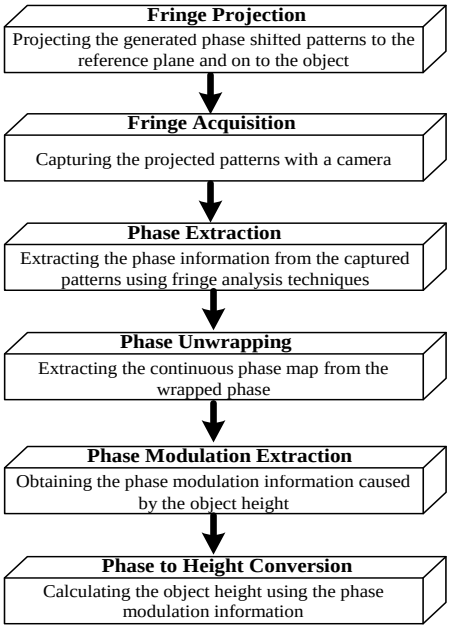

Figure 1: Flow Chart

In the digital fringe projection technique, the simple triangulation principle establishes the relationship between the unwrapped phase distribution and the geometric coordinates of the 3-D object. Using this relationship, the height can be obtained as a product of the calibration constant and the object shape-related phase component. The phase component can be obtained simply by subtracting the object phase from the reference phase. The calibration constant is a phase-to-height conversion constant that can be calculated from the parameters of the optical setup given below

a. Distance between the centre of the lens of the camera and that of the projector.

b. Distance between the camera projector plane and the reference plane.

c. Pitch of the pattern on the reference plane.

In practical conditions, however, it is very difficult to precisely measure system parameters, especially the fringe pitch, as it does not remain constant over the entire image plane due to the non telecentric projection [13]. In order to calculate the optical parameters precisely, the camera and the projector should be calibrated accurately but the projector calibration is usually a very complex and time-consuming task. To avoid this complexity, we introduced volumetric calibration, which makes use of calibration boards to calculate the calibration constant. The method is not only simple but it also produces accurate reconstructed 3-D geometry. Figure 1. shows a flowchart that describes the different steps involved in the measurement of the object's height using the digital fringe projection technique. A short description of each step is also given.

Section 2 presents the digital fringe projection method in details, including the photometric and volumetric calibration procedure and the height calculation of our scanning system. Section 3 describes the experiments and the results.

DIGITAL FRINGE PROJECTION

Phase-shifting technique: Many different phase-shifting algorithms have been developed by researchers, including the double three-step algorithm, three-step algorithm, four-step algorithm, least square algorithms, and Carré algorithm [14] [15] [16]. In this paper, the four-step phase-shifting algorithm is used. Four phase-shifted sinusoidal patterns with phase shift of 0, π/2, π, and 3π/2 are projected on to the object surface. Intensities of four images with phase shift of π/2 are given by

$$I_1(x,y) = a(x,y) + b(x,y)\cos\varphi(x,y) \quad (1)$$

$$I_2(x,y) = a(x,y) + b(x,y)\cos\left[\frac{\pi}{2} + \varphi(x,y)\right] \quad (2)$$

$$I_3 = a(x,y) + b(x,y)\cos[\pi + \varphi(x,y)] \quad (3)$$

$$I_4 = a(x,y) + b(x,y)\cos\left[\frac{3\pi}{2} + \varphi(x,y)\right] \quad (4)$$

where $a(x,y)$ is the average intensity, $b(x,y)$ is the intensity modulation, and $\varphi(x,y)$ is the phase to be determined. Solving (1) to (4) simultaneously, the phase is calculated as

$$\varphi(x,y) = arctan\frac{I_4(x,y)-I_2(x,y)}{I_1(x,y)-I_3(x,y)} \quad (5)$$

Phase unwrapping: The arc tangent function extracts the required phase information, but this information is in the range from -π to π along with discontinuities. In order to obtain the actual phase that is proportional to distance, these discontinuities need to be removed and the continuous phase distribution must be obtained. This process is known as phase unwrapping. Phase unwrapping appears simple but it is actually an extremely challenging task because of the errors in intensities that are caused by the electronic noise, background noise during data acquisition, abrupt phase changes caused by shadow or surface discontinuities, and low data modulation point caused by low surface reflectivity [17]. Also it is difficult to distinguish between genuine phase jumps and steps (or breaks) caused by object discontinuities. As a result of these unavoidable error sources, a simple unwrapping algorithm is unable to determine the continuous phase distribution. Different unwrapping algorithms have therefore been developed by researchers [18] [19] [20]. In this paper, the quality-guided phase unwrapping algorithm is used for unwrapping. The quality map that is required to guide the phase unwrapping algorithm is

obtained from the phase data itself. It guides the identification of significant discontinuities [21].

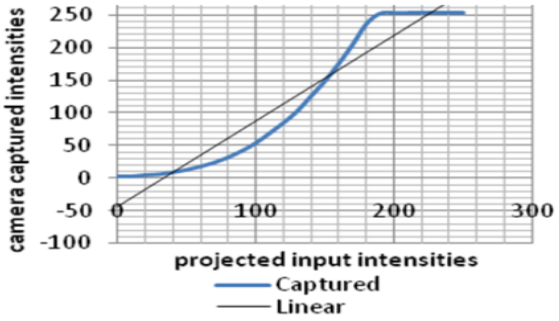

a. Projection response curve of projector

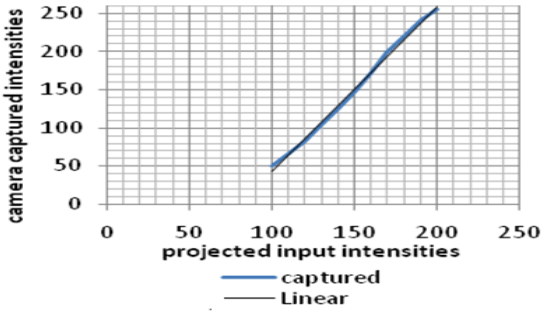

b. Projection response curve afet nonlinearity correction

Figure 2. Projection nonlinearity corrections

Photometric calibration: Photometric calibration is related to the calibration of intensity, which maps the captured intensity values to the projected intensity values. The projector response curve of a commercial video projector, which represents the relationship between intensities of the input pattern image and intensities of the image captured by the camera, is typically designed to be nonlinear for better visual effects.

Nonlinear projection is a source of phase measurement errors because it makes the intensity profile non-sinusoidal [21] [22]. In this research, a reverse lookup table (LUT) is built to reduce the effect of the nonlinearity of the projector. Figure 2(a) presents a typical projection response curve of the beam projector. It can be observed that, for input intensities less than 50 and greater than 200, there is no change in the output intensities and the range from 100 to 200 is quite linear so it is used in the experiments. The reverse LUT reduces the error made in the phase-stepping algorithm. The projection response curve is fitted using piecewise linearization. Figure 2(b) shows the projection response curve after nonlinearity correction. The curve exhibits linear behavior. A LUT is developed using the data from Figure 2(b). The LUT is used in a reverse mode to map the captured intensities to the corresponding projected intensities.

The nonlinearity errors in the projection response curve are compensated using the LUT. The projector response curve can never be truly linear, however, so it is difficult to completely eliminate these errors.

Phase-to-height conversion: Figure 3 depicts the optical geometry of the system used in the experiments. Point P and I are the centers of the lens of the beam projector and the charge-coupled device (CCD) camera. O is the point of intersection between the optical axis of the projector and the camera. From the CCD point of view, point D on the object has the same phase as point A on the reference plane. From the projector view-point, point D on the object has the same value as point C on the reference plane. It is assumed that P and I lie on the same plane, parallel to the reference plane. L is the distance between the two planes and d is the distance between P and I. Thus ΔACD and ΔIPD are similar and the following relationship can be established [23].

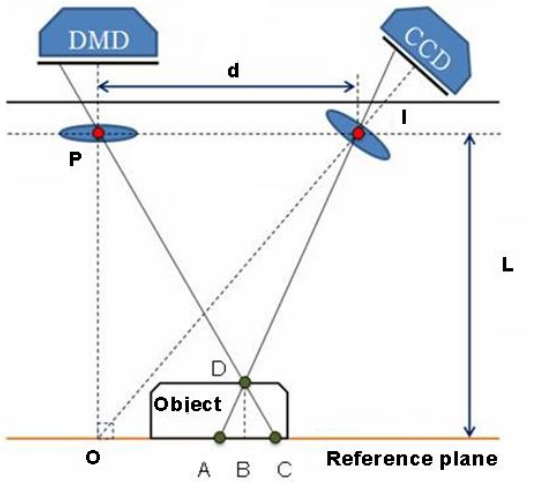

Figure 3. Optical geometry of fringe projection system

$$\frac{d}{\overline{AC}} = \frac{L-\overline{DB}}{\overline{DB}} = \frac{L}{\overline{DB}} - 1 \qquad (6)$$

If the distance between the two planes is large enough compared to the pitch of the projected pattern under normal view conditions,

$$\overline{DB} = \frac{AC\,(L-\overline{DB})}{d} = \frac{L\overline{AC}}{d} - \frac{\overline{DB}\;\overline{AC}}{d} \qquad (7)$$

$\overline{AC}$ is much smaller than d so we can neglect the last term of (7), and we get

$$\overline{DB} \approx \frac{L\overline{AC}}{d}$$

The relationship between distance $\overline{AC}$ on the reference plane and the phase change is give by (8)

$$\frac{\overline{AC}}{p} = \frac{\phi_{AC}}{2\pi} \qquad (8)$$

Replacing the distance $\overline{AC}$ by the corresponding phase change value, the height of the object is calculated as

$$z(x,y) = \overline{DB} = \frac{pL}{2\pi d}\phi_{AC} = K\phi_{AC} \quad (9)$$

where $z(x,y)$ is the height of the object at point D. (9) shows a phase-to-height conversion relationship where p is the pitch of the pattern on the reference plane, K is a calibration constant, and ϕ_{AC} is the phase change or phase modulation that is caused by the height of the object. This phase modulation can be expressed according to (8) as

$$\phi_{AC} = \frac{2\pi}{p}\overline{AC}$$

According to (5), let the calculated phase for the reference plane and object plane be $\varphi_r(x,y)$ and $\varphi_o(x,y)$. Using these two phase maps, the phase modulation information is calculated using the following equation.

$$\phi_{AC} = \varphi_o(x,y) - \varphi_r(x,y) \quad (10)$$

Phase-to-height conversion: In order to calculate the 3-D geometry of an object using an un calibrated projector, a measuring volume is defined. Figure 4 shows the basic setup of the 3-D scanning system, which consists of a CCD camera, a beam projector, and measuring volume. Measuring volume is defined in front of the reference plane. The phase-shifted patterns generated in the personal computer (PC) are projected by the projector, and captured by the CCD camera. On the reference plane, the projected fringe patterns act like the carrier pattern. The carrier pattern is the basic pattern that is used to carry the spatial deformation in a certain direction. When an object is placed on the reference plane, the phase of the carrier pattern is modulated by the height of the object. This modulated phase contains the object's depth information. The phase modulation information can be calculated using (10). The height of the object is reconstructed using the phase modulation information and the calibration constant. The calibration constant can be calculated from the parameters of the optical setup. These parameters are obtained by calibrating the projector, which is a complicated and time-consuming procedure. To avoid this complexity, the measuring volume is calibrated, which involves calculation of calibration constant. This is carried out using white calibration boards with known heights, as follow

a. Four sinusoidal phase-shifted patterns are projected on to the reference plane. The phase at the reference plane is calculated from the captured patterns using (5). Using the unwrapping algorithm, the continuous phase map is obtained.

b. A flat board with a known height h_1 (calibration board) is placed on the reference plane. The four phase-shifted patterns are projected on to this flat board. The continuous phase map for this board is then obtained using (5) and phase unwrapping.

c. Calibration boards with heights h_2, $h_{3,\ldots}$ h_n (n = 6 in our experimental setup) are placed on the reference plane. The continuous phase map is calculated in the same way for each board.

d. Phase modulation information is calculated by subtracting the reference plane's phase from the measured calibration boards' phase according to (10).

e. In this way the phase modulation information and the height of objects (calibration boards) is determined. Using these two known values, we can calculate the unknown value (calibration constant) in (9) as $K = z(x,y)/\phi_{AC}$. For n boards, the average value of the calibration constant can be calculated as $K = 1/n \sum_{i=1}^{n} K_i$ where K_i is the calibration constant for the i^{th} calibration board.

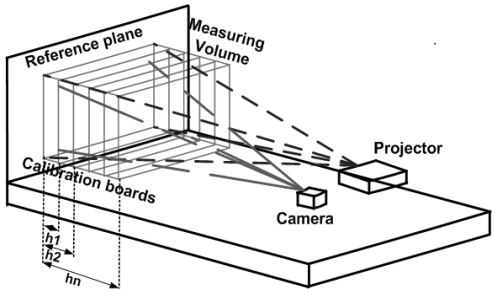

Figure 4. 3-D measurement system setup

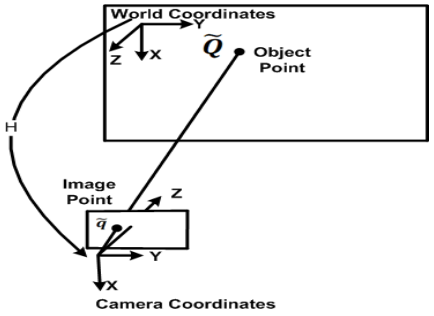

Figure 5. Relationship of image point to object point

The object to be measured is placed on the reference plane. Four phase-shifted patterns are projected on to the surface of the object. These patterns are captured with a camera and the phase value is calculated using (5). Phase modulation is calculated using (10). The height of the object is then calculated using the calibration constant and the phase modulation according to (9).

In order to calculate the x and y coordinates of the object, basic homography is used. As shown in Figure 5, point $\tilde{Q}$ is an object point on the reference plane that is seen as point $\tilde{q}$ on the camera image plane. Homography is induced between the reference plane

and the camera image plane. This linear mapping relates an object point to an image point as follows:

$$\tilde{q} = sH\tilde{Q} \quad (11)$$

where s is the scaling factor and H is homography, which maps the object points to image points [24]. Homography can be calculated from the camera's intrinsic and extrinsic parameters. The camera is accurately calibrated using Zhang's method [25]. (11) can be expressed as

$$\begin{bmatrix} x \\ y \\ 1 \end{bmatrix} = sH \begin{bmatrix} X \\ Y \\ 1 \end{bmatrix} \quad (12)$$

Thus, in order to extract the world coordinates of a point from a known image point data, the inverse homography matrix should be multiplied on both sides. The resultant matrix is then scaled down according to (14) to obtain the world coordinates

$$H^{-1}\begin{bmatrix} x \\ y \\ 1 \end{bmatrix} = \begin{bmatrix} sX \\ sY \\ s \end{bmatrix} \quad (13)$$

$$\tilde{Q} = \begin{bmatrix} X \\ Y \\ 1 \end{bmatrix} = \frac{1}{s}\begin{bmatrix} sX \\ sY \\ s \end{bmatrix} \quad (14)$$

Conversion from image coordinates to world coordinates is carried out using (12) to (14), where $H^{-1}$the inverse homography matrix and s is the scaling factor.

Measuring Volume Limitation: The measuring volume (maximum depth that the system can measure) has some limitations. In order to obtain the height from the phase modulation, the pitch p must be greater than $\overline{AC}$ in Figure 3 on the reference plane. If the pitch is smaller than $\overline{AC}$ we obtain the same phase values for two different points that are separated by p, and for two points at different heights, the calculated height will be the same. This phenomenon is explained in Figure 6. Consider three surfaces, S_1, S_2, and S_3. Let D_1, D_2, and D_3 be arbitrary points on surfaces S_1, S_2, and S_3, respectively. Let 'A' be a point of the reference plane. In the absence of any surface, it is captured as point A. Because of the heights of surfaces, instead of point A, points D_1, D_2, and D_3 will be projected on to a single pixel in the camera image plane. In order to calculate the height information at these arbitrary points, the phase modulation value at each point is calculated. Let $\varphi_A(x,y)$, $\varphi_{D1}(x,y)$, $\varphi_{D2}(x,y)$, and $\varphi_{D3}(x,y)$, be the phase value at point A, D_1, D_2, and D_3, respectively. According to (10), phase modulation for each point can be calculated as

At point D_1: $\phi_{AC1} = \varphi_{D1}(x,y) - \varphi_A(x,y)$

At point D_2: $\phi_{AC2} = \varphi_{D2}(x,y) - \varphi_A(x,y)$

At point D_3: $\phi_{AC3} = \varphi_{D3}(x,y) - \varphi_A(x,y)$

The obtained phase modulation value must be in the range [0-, 2π] and this value is repeated every 2π. This is due to the periodic nature of the sinusoidal pattern. If the distance $\overline{AC}$ on the reference plane exceeds the fringe period p, then it creates ambiguity. This phenomenon can be observed at point D_3 when the distance $\overline{AC_3}$ exceeds p. It can also be observed that point C_1 and C_3 are separated by p, i.e., $\overline{AC_3} = p + \overline{AC_1}$. This will cause the value at D_1 to repeat at D_3 and we will obtain the same phase modulation value for both points D_1 and D_3. As a result, the calculated height at both points will be the same. This phenomenon is also known as 2π ambiguity. The height of an object obtained using (9) is limited by K. As ϕ_{AC1} cannot exceed 2π, the maximum depth that can be measured is given by

$$z_{max}(x,y) = K\phi_{AC(max)} < 2\pi K \quad (15)$$

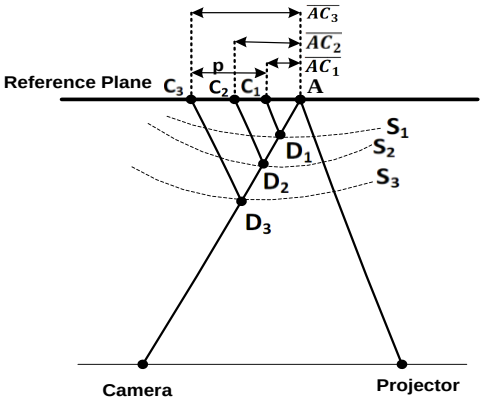

Figure 6. 2π ambiguity

EXPERIMENTS AND RESULTS

In the experimental demonstration, different objects were measured by the system to demonstrate the performance. Fringe patterns were generated by a computer and projected by an HS200 LG DLP projector. A CCD camera (UEYE) with 1024 × 768 resolutions and a 16 mm lens was used to capture the patterns. The software is written in visual C++ with the OpenCV library. An average value for the calibration constant is used for reconstruction.

A flat white board of 6 mm height was used to verify the system accuracy. The mean value of the measured flat surface is 6.02 mm and the standard deviation is approximately 0.318 mm.

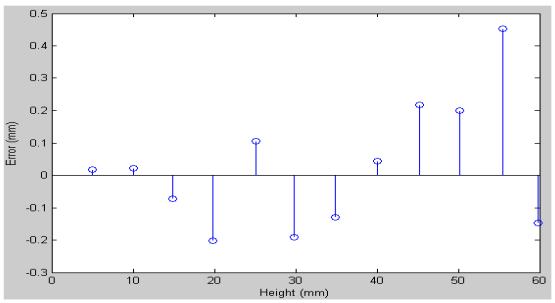

Figure 7. Measurement error

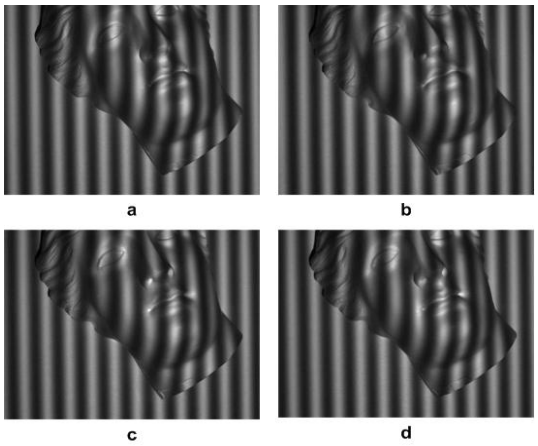

Figure 8. Projected and captured pattern on to the object surface

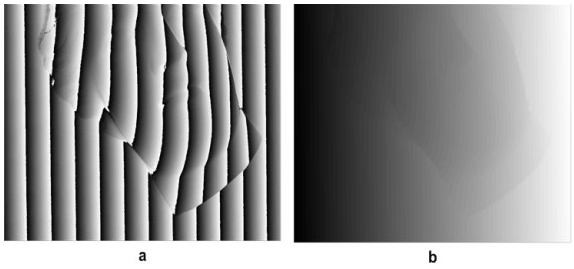

Figure 9. (a) Extracted phases (wrapped) (b) Unwrapped phase map

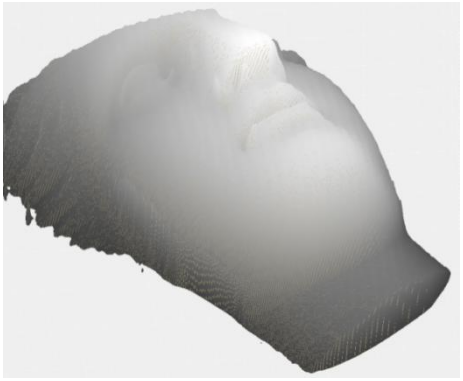

Figure 10. Reconstructed 3-D surface of the object

This shows that the system can measure the 3-D coordinates with a measurement error of 0.3 mm. Figure 8 shows the four captured phase-shifted sinusoidal patterns projected on to a sculpture. The extracted phase information and the unwrapped phase map are shown in Figure 9(a) and Figure 9(b), respectively. Figure 10 shows the reconstructed 3-D geometry. A mesh of the reconstructed surface is shown in Figure 11. In the experiments, it was observed that the higher the density of the projected pattern (i.e., the smaller the pitch), the more sensitive the measurement system. The quality of the fringe pattern also affects the accuracy and the phase errors can be effectively reduced by increasing the number of phase-shifted images.

Figure 11. Reconstructed object (mesh)

CONCLUSION

A simple method based on fringe projection for reconstruction of the 3-D geometry of an object is proposed. This method provides easy implementation by avoiding the complex and time-consuming process of projector calibration. The measuring volume is calibrated using flat white boards. 3-D geometry is reconstructed using an un calibrated projector and calibration boards with known depth. This method requires a video projector and a calibrated camera only. This method does not require a cumbersome optical setup. The 3-D measuring process is fast and object coordinates are reconstructed with high resolution. Various object surfaces were used for the experiments. The standard deviation of the measuring error is approximately 0.3 mm. This system can be used as a fundamental system and starting point for students and researchers in the field of 3-D reconstruction.

ACKNOWLEDGMENT

This work was supported in part by the Korea Ministry of Knowledge Economy, under Grant of the Strategic Technology Development Project on Biomedical Supplier (Development of the Digital Fusion Artificial Tooth Treatment Supporting System). This paper is a result of research during the 1st and 2nd author's Master degree program at Myongji University.

Corresponding Author:
Kang Park, Dept. of Mechanical Engineering, Myongji University, Yongin,Gyeonggi-Do, South Korea
Email: kang@mju.ac.kr

REFERENCES

[1] Li, Y. F. and Lu, R. S., "Uncalibrated Euclidean 3-D Reconstruction Using an Active Vision System," IEEE Transaction on Robotics and Automation, Vol. 20, pp. 15-25, 2004.

[2] Yingsong Hu, Jiangtao Xi, Enbang Li, Joe Chicharo, and Zongkai Yang, "Three-dimensional profilometry based on shift estimation of projected fringe patterns", Applied Optics, Vol. 45, pp. 678-687, 2006.

[3] Kazuyuki Miyazawa and Takafumi Aoki, "A Robot-Based 3-D Body Scanning System Using Passive Stereo Vision," 15th IEEE International Conference on Image Processing, pp. 305-308, 2008.

[4] Naohide Uchida, Takuma Shibahara, Takafumi Aoki, Hiroshi Nakajima and Koji Kobayashi, "3-D Face Recognition Using Passive Stereo Vision," IEEE International Conference on Image Processing, Vol. 2, 2005.

[5] Carlos Diaz and Leopoldo Altamirano, "Dense 3-D Surface Acquisition Using Projected Fringe Technique," Proc. of the Fifth Mexican Int. Conf. in Computer Science, pp. 116-123, 2004.

[6] Li Zhang and Kazem Alemzadeh, "A 3-Dimensional Vision System for Dental Applications," Proc. of the 29th Annual Int. Conf. of the IEEE EMBS, pp. 3369-3372, 2007.

[7] Bouguet, J.Y. and Perona, P. "Method For Recovering 3-D Surface Shape Based On Grayscale Structured Lightning," http://www.vision.caltech.edu/bouguetj/.

[8] Joaquim Salvi, Jordi Pages and JoanBatlle, "Pattern codification strategies in structured light systems," Pattern Recognition, Vol. 37, pp. 827-849, 2004.

[9] LI Yao, Lizhuang Ma, Zuoyong Zheng and Di wu, "A Low Cost 3-D Shape Measurement Method Based on a Strip Shifting Pattern," ISA Transactions, Vol. 46, pp. 267-275, 2007.

[10] Ryu, Weon-Jae; Kang, Young-June; Baik, Sung-Hoon; Kang and Shin-Jae, "A Study on the 3-D Measurement By Using Digital Projection Moiré Method," Optik, Vol. 119, pp. 453-458, 2008.

[11] Asundi, A. and Yung, K. H. "Phase-shifting and Logical Moiré," Optical Society of America, Vol. 8, pp. 1591-1600, 1991.

[12] Lu, C., Yamaguchi, A. and Inokuchi, S. "Intensity Modulated Moiré and its Intensity-Phase Analysis," Fourteenth International Conference on Pattern Recognition, vol.2, pp. 1791-1793, 1998.

[13] Xiaobo, C., Tong, X. J., Tao, J. and Ye, J. "Research and Development of an Accurate 3-D Shape Measurement System Based on Fringe Projection," Precision Engineering, Vol. 32, pp. 215-221, 2008.

[14] Da, F. and Gai, S. "Flexible Three-Dimensional Measurement Technique Based on a Digital Light Processing Projector," Applied Optics, Vol. 47, No. 3, pp. 377-385, 2008.

[15] Huang, P. S., Hu, Q. J. and Chiang, F. P. "Double Three-Step Phase Shifting Algorithm," Applied Optics, Vol. 41, No. 22, pp. 4503-4509, 2002.

[16] Schreiber, H. and Bruning, J. H. "Phase Shifting Interferometry," in Optical Shop Testing, 3rd Edition, John Wiley & Sons, pp. 547-654, 2007.

[17] Diaz, C. and Altamirano, L. "Fast Non-continuous Path Phase-Unwrapping Algorithm Based on Gradients and Mask," Springer, Vol. 3287, pp. 116-123, 2004.

[18] Qian, K., Soona, S. H. and Asundi, A. "A Simple Phase Unwrapping Approach Based on Fltering by Windowed Fourier Transform," Optics & Laser Technology, Vol. 37, pp. 458-462, 2005.

[19] Su, F., Yi, S. and Chian, K. S. "A Simple Method to Unwrap the Geometrically Discontinuous Phase Map and its Application in the Measurement of IC Package," Optics and Lasers in Engineering, Vol. 41, pp. 463-473, 2004.

[20] Bioucas-Dias, J. M. and Valadão, G. "Phase Unwrapping via Graph Cuts," IEEE Transactions on Image Processing, 2007.

[21] Zhang, S. and Huang, P. S. "Phase Error Compensation for a 3-D Shape Measurement System Based on the Phase Shifting Method," Optical Engineering, Vol. 46(6), No. 063601, 2007.

[22] Li, Z. W., Shi, Y., Wang, C. and Wang, Y. "Accurate Calibration Method for a Structured Light System," Optical Engineering, Vol. 47(5), No. 053604, 2008.

[23] Zhang, S. "High-resolution, Real-time 3-D Shape Measurement," PhD Thesis, Mechanical Engineering, Stony Brook University, 2005.

[24] Bradski, G. and Kaehler, A. "Learning OpenCV," O'Reilly Media, Inc., pp. 370-400, September 2008.

[25] Zhang, Z. "Flexible Camera Calibration by Viewing a Plane from Unknown Orientation," International Conference on Computer Vision, ICCV'99, pp. 666-673, 1999.

6/4/2013